JCTC Journal of Chemical Theory and Computation

First Principles Study of NO and NNO Chemisorption on Silicon Carbide Nanotubes and Other Nanotubes

Guohua Gao† and Hong Seok Kang*

Department of Nano and Advanced Materials, College of Engineering, Jeonju University, Hyoja-dong, Wansan-ku, Chonju, Chonbuk 560-759, Republic of Korea

Received June 8, 2008

Abstract: Using methods based on first principles, we find that NO and NNO molecules can be chemisorbed on silicon carbide nanotubes (SiCNTs) with an appreciable binding energy and that this is not the case for either carbon nanotubes (CNTs) or boron nitride nanotubes (BNNTs). A detailed analysis of the energetics, geometry, and electronic structure of various isomers of the complexes was performed. The adsorption energy (∼−0.7 eV) is larger for the SiCNT-NO complex. The complex exhibits magnetism, and a ferromagnetic coupling of spins is observed when more than one NO molecule is adsorbed. This observation suggests that magnetic properties can be used to sense the amount of NO molecules adsorbed. The SiCNT-NNO complex is a nonmagnetic system in which five-membered rings form at the binding site.

1. Introduction

Among the many materials for semiconductors, bulk SiC has been found to be potentially useful for high power, high frequency, and high temperature electronic devices.[1] Therefore, motivated by the recent discovery of carbon nanotubes (CNTs), studies have sought to synthesize tubular forms of SiC. SiC nanotubes (SiCNTs) have been successfully synthesized from the reaction of SiO and multiwalled CNTs.[2] In SiCNTs, carbon and silicon atoms exist in a 1:1 ratio, and a theoretical calculation shows that the tubes consist of alternating C and Si atoms forming sp^2 Si−C bonds.[3] Single-walled SiCNTs are known to be semiconductors irrespective of their chiral indices, because of the ionicity of Si−C bonds. The tubes are expected to be amenable to a variety of external functionalizations due to the presence of the Si atoms, which prefer sp^3 hybridization. In fact, the exterior surface of SiCNTs is much more reactive than the exterior of either CNTs or boron nitride nanotubes (BNNTs), making SiCNTs much more interesting for chemical functionalization than the other type of nanotubes. For example, transition metal atoms can be chemically adsorbed on SiCNTs with binding energies greater than 1.17 eV.[4] SiCNTs have also proven useful for hydrogen storage, since the binding energy of the tubes with hydrogen molecules is 20% larger than that of CNTs.[5]

Nitrogen oxides (NOx) are compounds notorious for their harmful impact on the environment. They are mostly generated as byproducts of high-temperature combustion of fossil fuels.[6] Although there have been many efforts to use catalysts to reduce the amount of nitrogen oxides in the air,[7] an efficient method of sensing and removing the pollutants is still needed. Very recently, $SnO_2-In_2O_3$ nanocomposites have been shown to be useful as semiconductor NOx sensors, since they can selectively and reproducibly detect the gases at the level of parts-per-million.[8] Heme-nitric oxides, which constitute a newly discovered family of heme proteins, have also been found to detect the molecules selectively and sensitively.[9] Nanocrystalline titanium dioxide is known to be useful for photocatalytic degradation of the molecules.[10]

These results prompted us to take a theoretical approach to ask whether nanotubes could be used for this purpose, particularly in light of the high chemical reactivity of SiCNTs. To our knowledge, there has been only one theoretical work related to that problem: Rafati et al. found that an NO molecule can be physisorbed on the surface of CNTs endothermically.[11] Nevertheless, recent quantum chemical calculations have elucidated the mechanism of reaction of tungsten with NOx.[12] There has been an

* Corresponding author e-mail: hsk@jj.ac.kr.

† Alternate address: Pohl Institute of Solid State Physics, Tongji University, Shanghai 200092, P. R. China.

10.1021/ct800273c CCC: $40.75
Published on Web 09/12/2008

investigation of the structure and energetics of NOx adsorption on clusters[13] and studies of NOx binding on various surfaces.[14]

The present work is devoted to a first-principles investigation of using SiCNTs as a sensor and adsorbent of NO and NNO molecules. The study also compares the adsorption performance of SiCNTs, CNTs, and BNNTs.

2. Theoretical Methods

Total energy calculations were performed using the Vienna *ab initio* simulation package (VASP).[15,16] Electron-ion interactions were described by the projected augmented wave (PAW) method.[17] Exchange-correlation effects were treated within the generalized gradient approximation (GGA) of Perdew, Burke, and Ernzerhof.[18] The cutoff energy was set high enough (400 eV) to ensure accurate results, and the conjugate gradient method was employed to optimize the geometry until the Hellmann−Feynman force exerted on an atom was less than 0.03 eV/Å.

In order to investigate differences in adsorption properties of armchair and zigzag tubes, we examined supercells, which consisted of three and four primitive cells of (8,0) and (5,5) nanotubes, respectively. Although we focused on SiCNTs, we also analyzed CNTs and BNNTs for the purposes of comparison. The total number of atoms, the diameter, and the lattice parameter were (80, 8.62 Å, 12.39 Å) and (96, 8.06 Å, 16.02 Å) for (5,5) and (8,0) SiCNTs, respectively. The corresponding parameters for (5,5) CNT, (8,0) CNT, (5,5) BNNT, and (8,0) BNNT were (80, 6.87 Å, 9.90 Å), (96, 6.46 Å, 12.78 Å), (80, 7.00 Å, 9.90 Å), and (96, 6.58 Å, 12.90 Å), respectively. Here, lattice parameters are optimized values in such a way that the axial stress is zero. Two *k*-points were used for *k*-point sampling in the irreducible region of the first Brillouin zone along the tube axis (X), which ensures the accuracy of the calculation within 1 meV even for metallic systems. In these analyses, we used large supercells to guarantee that interatomic distances between neighboring cells along the Y and Z directions were greater than 10.3 Å.

3. Results

First, we investigated NO adsorption on the surface of nanotubes. We describe our calculations on three different configurations of the NO molecule on a SiCNT of a specific chiral index (*n, m*). In Table 1, these configurations are denoted (E, Z, Z^R) and (Z, A, Z^R) for (5,5) and (8,0) SiCNTs, respectively. As shown in Figure 1 the letters Z, E, and A indicate whether the NO molecule is located directly above the zigzag, equatorial, or axial Si−C bond, respectively. A zigzag bond is defined as a bond that is neither parallel nor perpendicular to the tube axis. An equatorial bond is perpendicular to the tube axis, while an axial bond is parallel to the axis. We note that there are no axial bonds in armchair tubes and no equatorial bonds in zigzag tubes. In the E, Z, and A configurations, the oxygen atom, which is more electronegative than the nitrogen atom in the NO molecule, is located directly above a silicon atom (Si_1), which is more electropositive than carbon atoms. Likewise, the nitrogen atom is located directly above a carbon atom (C_1) that is bonded to Si_1. Therefore, there can be N−C_1 and O−Si_1 bonds. On the other hand, in configuration Z^R, the nitrogen atom is located above the silicon atom of a zigzag bond, so there can be O−C_1 and N−Si_1 bonds instead.

Table 1. Energetic, Magnetic, and Geometric Parameters for Various Configurations of SiCNT-NO Complexes in Which the SiCNTs Have (5,5) and (8,0) Chiral Indices

	chiral index					
	(5,5)			(8,0)		
configuration	E	Z	Z^R	Z	A	Z^R
$E_b(1)$[a] (eV)	−0.67	−0.63	0.82	−0.62	−0.61	0.69
$E_b(2)$[b] (eV)		−1.54		−1.41		
$\mu(1)$[c] (μ_B)	1.00	0.95	1.00	0.92	1.00	1.00
$\mu(2)$[d] (μ_B)		1.98		2.00		
l (N−C_1)[e] (Å)	1.50	1.49	1.54	1.48	1.52	1.51
l (O−Si_1)[f] (Å)	1.75	1.80	1.83	1.79	1.76	1.81
l (N−Si_2)[g] (Å)	2.78	1.93	3.00	1.98	2.73	2.69
l (C_1−Si_1)[h] (Å)	1.98 (1.79)	1.90 (1.79)		1.92 (1.79)	1.91 (1.79)	
l (O−N)[i] (Å)	1.40 (1.17)	1.40 (1.17)	1.39 (1.17)	1.40 (1.17)	1.40 (1.17)	1.39 (1.17)
q(NO)[j]	−0.48 (0)	−0.51 (0)		−0.52 (0)	−0.46 (0)	

[a] Binding energy of one NO molecule on the surface of the SiCNT. [b] Binding energy of two NO molecules on the surface of the SiCNT. [c] Magnetic moment of the SiCNT-NO complex with one NO molecule adsorbed. [d] Magnetic moment of the SiCNT-NO complex with two NO molecules adsorbed. [e] N−C_1 distance, where C_1 is the carbon atom of the SiCNT above which the nitrogen atom of the NO molecule is located. For configuration Z^R, the number corresponds to the O−C_1 distance instead. [f] O−Si_1 distance, where Si_1 is the silicon atom of the SiCNT above which the oxygen atom of the NO molecule is located. For configuration Z^R, the number corresponds to the N−Si_1 distance instead. [g] N−Si_2 distance, where Si_2 is a silicon atom of the SiCNT in the bonds Si_1−C_1−Si_2 of the SiCNT. For configuration Z^R, the number corresponds to the O−Si_2 distance. [h] C_1−Si_1 bond length. The numbers in parentheses denote the corresponding data in pristine tubes. [i] N−O bond length in the NO molecule. [j] Total Mulliken charge of the NO molecule. The numbers in parentheses denote the corresponding data for an isolated NO molecule.

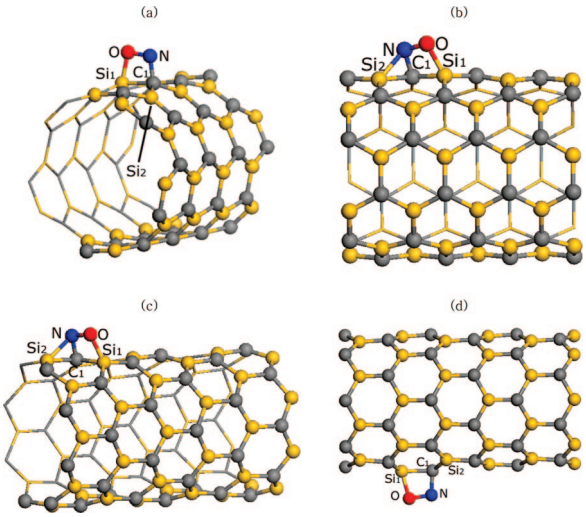

Figure 1. Optimized structures for stable configurations of SiCNT-NO complexes: configurations E (a) and Z (b) of the (5,5) complex and configurations Z (c) and A (d) of the (8,0) complex. Atomic labels are also defined.

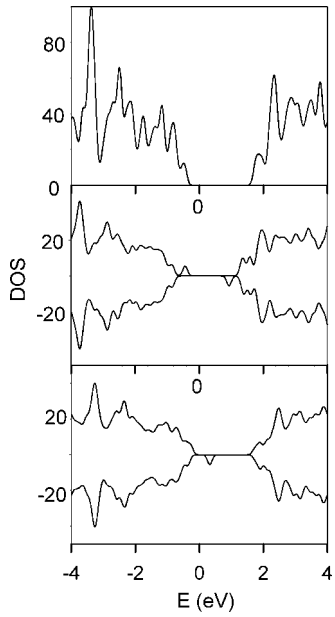

Figure 2. Comparison of the electronic density of states (DOS) for (5,5) SiCNT-NO complexes: pristine tube (top), configuration E (middle), and configuration Z (bottom). The Fermi level is set to zero. For the complex, DOSs for spin-up and spin-down states are drawn separately.

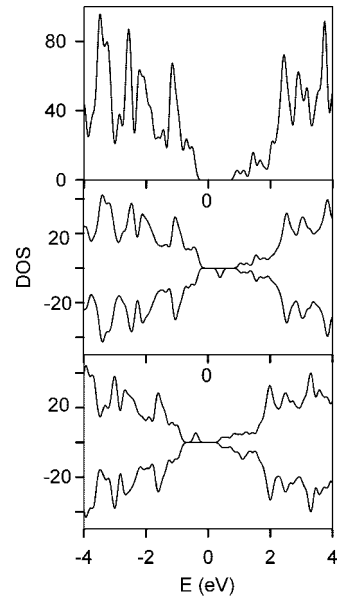

Figure 3. Comparison of the electronic density of states (DOS) for (8,0) SiCNT-NO complexes: pristine tube (top), configuration Z (middle), and configuration A (bottom). The Fermi level is set to zero. For the complex, DOSs for spin-up and spin-down states are drawn separately.

Table 1 shows that there is appreciable binding between an NO molecule and SiCNTs in configurations E, Z, and A. In fact, the magnitude of the binding energy or adsorption energy (E_b) of an NO molecule, which is defined as the energy change associated with the process SiCNT + NO(doublet) → NO-SiCNT, is between −0.61 and −0.67 eV for (5,5) and (8,0) SiCNTs. We do not observe any significant difference in binding energy between the tubes of two different chiral indices. Table 1 and Figures 2 and 3 show that the NO-SiCNTs are magnetic semiconductors with magnetic moments close to 1.0 μ_B.[19] A separate analysis shows that the spin polarization is largely concentrated on the NO molecule. As two examples, Figure 4 shows the spin density distributions of configuration E of (5,5) and configuration Z of (8,0) SiCNT-NO complexes depicted in Figure 1(a),(c).

When two NO atoms are adsorbed, the binding of the second NO molecule is stronger than the first one, indicating that the NO binding is cooperative. For example, Table 1 shows that the adsorption energy of the first and the second NO molecules for isomer Z of (5,5) SiCNTs is −0.63 eV and −0.91 eV, respectively. Spins of two NO molecules couple ferromagnetically, resulting in magnetic moments of 2.0 μ_B for both of (5,5) and (8,0) tubes. In order to estimate the coupling strength between local magnetic moments of two NO molecules, we have calculated the energy difference ($\Delta E_{F\text{-}AF}$) between ferromagnetic and antiferromagnetic states from the relation: $\Delta E_{F\text{-}AF} = E_F - E_{AF}$. Its values (= −0.16 eV and −0.35 eV, respectively) show that there are strong couplings between local magnetic moments for both of (5,5) and (8,0) complexes, suggesting the possibility of long-range magnetic ordering at room temperature.

As Figure 5 shows, the second NO molecule is adsorbed on the nearest carbon atom of the tubes in the most stable

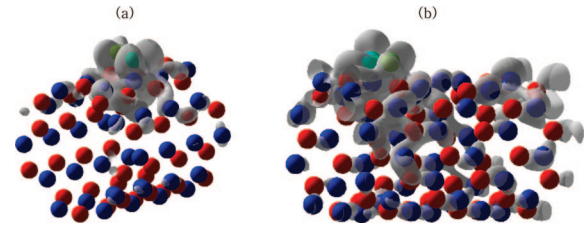

Figure 4. Spin density plot of configuration E (a) of (5,5) and configuration Z (b) of (8,0) SiCNT-NO complexes, in each of which the tube has the same orientation as in Figure 1(a) and (c).

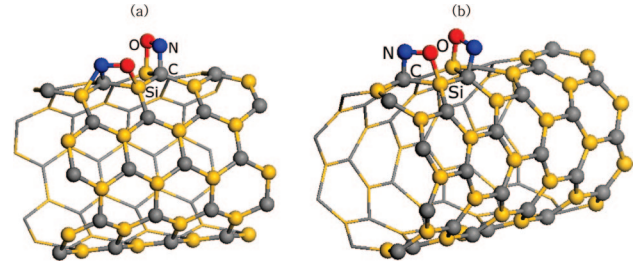

Figure 5. Optimized structures of (5,5) (a) and (8,0) (b) SiCNT-2NO complexes.

configuration. Namely, two NO molecules are found to be adsorbed on C_1 and C_2 in the bonds C_1-Si-C_2 of the tube. In the figure, two NO molecules adopt E and Z configurations, respectively, for the (5,5) complex. For the (8,0) complex, both of them adopt Z configurations. The configurations are more stable than another configuration by 0.26 and 0.14 eV for (5,5) and (8,0) tubes, respectively, in which two NO molecules are located far away on the opposite sides of the circumference of the tube. Therefore, the change in the magnetic moment of SiCNTs can be used to sense the amount of NO gas adsorbed. As shown in Table 1, Z^R

Scheme 1. Schematic Energy Level Diagram of Two π^* Molecular Orbitals of the NO Molecule before and after Adsorption on Isomer E of (5,5) SiCNT

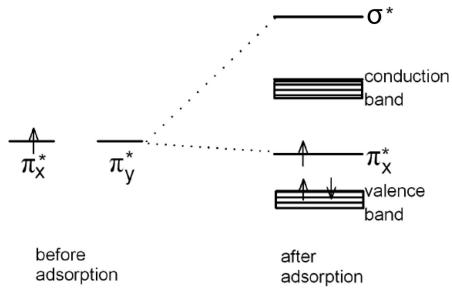

configurations are not expected to be observable in either (5,5) or (8,0) tube, since the binding energy is largely positive. Therefore, we concentrate our work on configurations E, Z, and A.

As was mentioned in the previous paragraph, Figure 1 shows the molecular structure of SiCNTs with one NO molecule adsorbed on the surface for configurations E and Z of the (5,5) complex and Z and A of the (8,0) complex. The N−C_1 bond length is 1.49−1.52 Å, almost achieving the length of a single covalent bond.[20] There is an O−Si_1 bond that is somewhat weaker than a single bond, as indicated by its bond length (1.75−1.80 Å), which is longer than that (1.66 Å) of an Si−O single bond.[19] As a result, the C_1−Si_1 and N−O bonds are appreciably weakened, which is seen in their bond lengths (1.90−1.98 Å and 1.39−1.40 Å, respectively), which are longer than those in pristine tubes (1.79 Å) and an isolated NO molecule (1.17 Å). In fact, comparison of the length of the N−O bond in the adsorbed molecule with the lengths of single and double N−O bonds indicates that the bond order changes from 2.5 to 1. There are also weak N−Si_2 bonds in the Z configuration of both (5,5) and (8,0) tubes, which is not the case in other configurations.

In order to better understand the electronic properties of the complex, we used the E configuration of the (5,5) complex as an example. (We recall that the X-axis is parallel to the tube axis. For armchair tubes, we also assume that the equatorial direction of the NO molecule is parallel to the Z-axis. Therefore, the π orbitals of the tube are directed along the Y-axis.) Let us assume the electronic configuration ($2\pi_x^{*1}$, $2\pi_y^{*0}$) in an isolated NO molecule. Our analysis of *l,m*-projected local density of states (LDOS) shows that the $2\pi_x$*(NO) orbital does not interact significantly with tube states, that it remains half-filled, and that it contributes to the spin polarization of the complex. $2\pi_y$*(NO), which is degenerate with $2\pi_x$*(NO) in an isolated NO molecule, is now located above the conduction band edge. [See Scheme 1.] This is because it becomes a σ* orbital for the O−Si_1 and N−C_1 bonds. In short, the spin polarization of the complex can be attributed to that in the π*(NO) orbital, which is perpendicular to the N−C_1 and O−Si_1 bonds.

Figures S1 and S2 show the change of the band structure after the adsorption of one and two NO molecules. As was mentioned in the previous paragraph, a new state is introduced in the band gap of the pristine SiCNT when one NO molecule is adsorbed, which is $2\pi_x$*(NO) state weakly

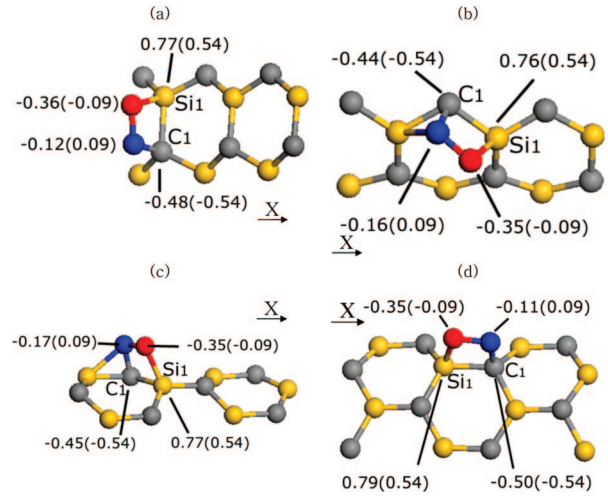

Figure 6. Mulliken charges of atoms around the adsorption site for SiCNT-NO complexes depicted in Figure 1: configurations E (a) and Z (b) of the (5,5) tube and configurations Z (c) and A (d) of the (8,0) tube. For the better understanding, the former two figures, (a) and (b), are rotated along the tube axis (= X), while others have the same orientations as in Figure 1.

interacting with a π(tube) state. This state is located below the Fermi level for the spin-up state. On the other hand, it is located above the Fermi level for the spin-down state, causing the spin-polarization of the complex. When two NO molecules are adsorbed, two $2\pi_x$*(NO) states are introduced from two NO molecules. As a result, the band gap of the system decreases from those of pristine SiCNTs after the adsorption. However, Figures S1 and S2 indicate that there is no definite trend in the change of the gap as a function of NO molecules adsorbed.

A separate PBEPBE/6−31G(d) calculation using the GAUSSIAN03 program shows that both the N and O atoms have negative values of the Mulliken charge. For example, the charges are −0.12 and −0.36, respectively, in the E configuration of the (5,5) SiCNT. Upon complex formation, there is a net charge transfer of 0.46−0.52*e* from the tube to the molecule. Figure 6 shows Mulliken charges of atoms around the adsorption site for configurations of (5,5) and (8,0) SiCNT-NO complexes depicted in Figure 1. It shows that approximately one-half of the transferred electrons come from Si_1.

Figure S3 shows four other initial configurations of the (5,5) SiCNT-NO complex considered in this work. In configuration H1, which corresponds to S3(a), we built an initial O−Si_1 bond perpendicular to the tube surface. Similarly, we introduced an initial N−C_1 bond perpendicular to the tube surface in configuration H2. In configurations H3 and H4, which correspond to Figure S3(c),(d), the NO molecule is located diagonal to a hexagon of the tube. In all of them, initial bond lengths of O−Si and N−C bonds were chosen to be similar to those in stable configurations shown in Table 1. Two of them, which correspond to configurations H3 and H4, result in the same final structure in which the NO molecule is chemisorbed in such a way that a Si−N bond is formed. [See Figure S4(a).] However, its binding energy (= −0.34 eV) is smaller than those of configurations E and Z shown in Table 1. This is manifested in the Si−N

Table 2. Energetic and Geometric Parameters for Various Configurations of CNT-NO and BNNT-NO Complexes in Which the Nanotubes Have (5,5) and (8,0) Chiral Indices

	CNT				BNNT			
	(5,5)[e]		(8,0)[e]		(5,5)[e]		(8,0)[e]	
configuration	E	Z	Z	A	E	Z	Z	A
E_b[a] (eV)	2.07	2.08	2.03	1.71	1.59	1.77	1.62	1.57
l (O−C_1)[b] (Å)	1.49	1.55	1.53	1.52	1.52	1.58	1.56	1.56
l (N−C_2)[c] (Å)	1.49	1.50	1.49	1.49	1.51	1.58	1.53	1.57
l (O−N)[d] (Å)	1.39	1.37	1.39	1.38	1.35	1.34	1.35	1.35
	(1.17)	(1.17)	(1.17)	(1.17)	(1.17)	(1.17)	(1.17)	(1.17)

[a] Binding energy of one NO molecule on the surface of the CNT and BNNT. [b] O−C_1 distance, where C_1 is the carbon atom of the CNT above which the oxygen atom of the NO molecule is located. In BNNT-NO complexes, C_1 denotes a boron atom of the BNNT instead. [c] N−C_2 distance, where C_2 is the carbon atom of the CNT bonded to C_1 above which the nitrogen atom of the NO molecule is located. In BNNT-NO complexes, C_2 denotes a nitrogen atom of the BNNT instead. [d] N−O bond length in the NO molecule. The numbers in parentheses denote the corresponding length in an isolated molecule. [e] Chiral index.

bond length (=2.02 Å) which is appreciably larger than Si−O bond lengths (∼1.80 Å) in configurations E and Z. Relaxations of other initial structures result in physisorption ($|E_b| < 0.1$ eV) in which no chemical bond is formed between the tube and the NO molecule.

Figure S5 also shows four other initial configurations (=G1−G4) of the (8,0) SiCNT-NO complex, each of which is characterized by the geometrical feature which is the same as the corresponding one for the (5,5) complex already described. Only configurations G3 and G4 result in the chemisorption ($E_b = -0.37$ eV) shown in Figure S4(b), in which the local geometry around the adsorption site is similar to that of configuration H3 of the (5,5) complex.

Now we investigate the adsorption of an NO molecule on CNTs and BNNTs. In contrast to SiCNTs, these nanotubes exhibit highly endothermic binding to NO, which is even more pronounced for CNTs (Table 2). These binding energy data predict that the chemisorption of NO molecules is practically impossible on these tubes. A separate calculation shows that there are barriers for the desorption of the NO molecule in all the configurations of the complex, indicating that the complex indeed corresponds to a metastable state. This observation suggests that barriers for the adsorption are much higher than the value (=0.026 eV) of kT at room temperature. In fact, our separate calculation shows that the barriers for the adsorption are greater than 1.86 and 1.67 eV for configuration E of (5,5) and configuration A of (8,0) of CNT-NO complexes. Similarly, corresponding barriers for BNNT-NO complexes are greater than 1.40 and 1.32 eV, respectively.

Table 2 shows that upon adsorption of the NO molecule on CNTs, the O−C_1 and N−C_2 bonds that form are weaker than single bonds. (Here, C_1 and C_2 correspond to the carbon atoms of CNTs bonded to each other and on which the NO molecule sits.) The O−N bond of the NO molecule is also weakened to a single bond. A similar analysis holds for the complex involving BNNTs. We want to recall that our calculation is focused on the chemisorption of the molecule, not on its physisorption as was recently investigated by Rafati et al.[11] This difference is manifested in the O−C_1 distance (1.49−1.55 Å) of the CNT-NO complex obtained from our calculation, which is much shorter than that (∼3.15 Å) from their calculation.

Next, we examine the adsorption of an NNO molecule on the surface of SiCNTs. Table 3 shows the binding energy of the molecule in various configurations. In the E, Z, and A configurations, there is appreciable NNO-SiCNT binding, although this is weaker than for the NO molecule. Figure 7 shows that these configurations are characterized by the formation of five-membered rings around the equatorial, zigzag, and axial adsorption sites, depending on the configuration. (Note that atoms in the molecule N_1−N_2−O are labeled N_1, N_2, and O.) This ring formation is achieved by (1) the formation of O−Si_1 and N−C_1 single bonds, (2) bending of the N_1−N_2−O bond in such a way that the linear configuration of the isolated molecule is destroyed, and (3)

Table 3. Energetic and Geometric Parameters for Various Configurations of SiCNT-NNO Complexes in Which the SiCNTs Have (5,5) and (8,0) Chiral Indices

	chiral index					
	(5,5)			(8,0)		
configuration	E	Z	C	Z	A	C
$E_b(1)$[a] (eV)	−0.44	−0.40	0.66	−0.43	−0.56	0.56
E_{gap}[b]	1.99	1.84		1.33	1.29	
	(2.18)	(2.18)		(1.35)	(1.35)	
l (N_1−C_1)[c] (Å)	1.52	1.52		1.52	1.51	
l (O−Si_1)[d] (Å)	1.75	1.74		1.75	1.74	
l (C_1−Si_1)[e] (Å)	1.96	1.93		1.95	1.93	
	(1.79)	(1.79)		(1.79)	(1.79)	
l (N_1−N_2)[f] (Å)	1.25	1.25		1.25	1.25	
	(1.15)	(1.15)		(1.15)	(1.15)	
l (N_2−O)[g] (Å)	1.39	1.40		1.39	1.41	
	(1.20)	(1.20)		(1.20)	(1.20)	
θ(N_1−N_2−O)[h]	117.4	117.0		117.3	117.1	
	(180)	(180)		(180)	(180)	
q (NNO)[i]	−0.48	−0.48		−0.49	−0.47	
	(0)	(0)		(0)	(0)	

[a] Binding energy of one NNO molecule on the surface of the SiCNT. [b] The band gap of the SiCNT-NNO complex. [c] N_1−C_1 distance, where C_1 is the carbon atom of the SiCNT above which N_1 is located. Two nitrogen atoms of the NNO molecule are defined by the bonds N_1−N_2−O. [d] O−Si_1 distance, where O is the oxygen atom of the NNO molecule. Si_1 is the silicon atom of the SiCNT bonded to C_1 above which O is located. [e] C_1−Si_1 bond length. The numbers in parentheses denote the corresponding data in pristine tubes. [f] N_1−N_2 bond length of the NNO molecule. The numbers in parentheses denote the corresponding data for an isolated molecule. See footnote *c* for the definitions of N_1 and N_2. [g] N_2−O bond length of the NNO molecule. The numbers in parentheses denote the corresponding data in an isolated molecule. See footnote *c* for the definition of N_2. [h] Bond angle of the NNO molecule. [i] Total Mulliken charge of the NNO molecule. The numbers in parentheses denote the corresponding data in an isolated molecule.

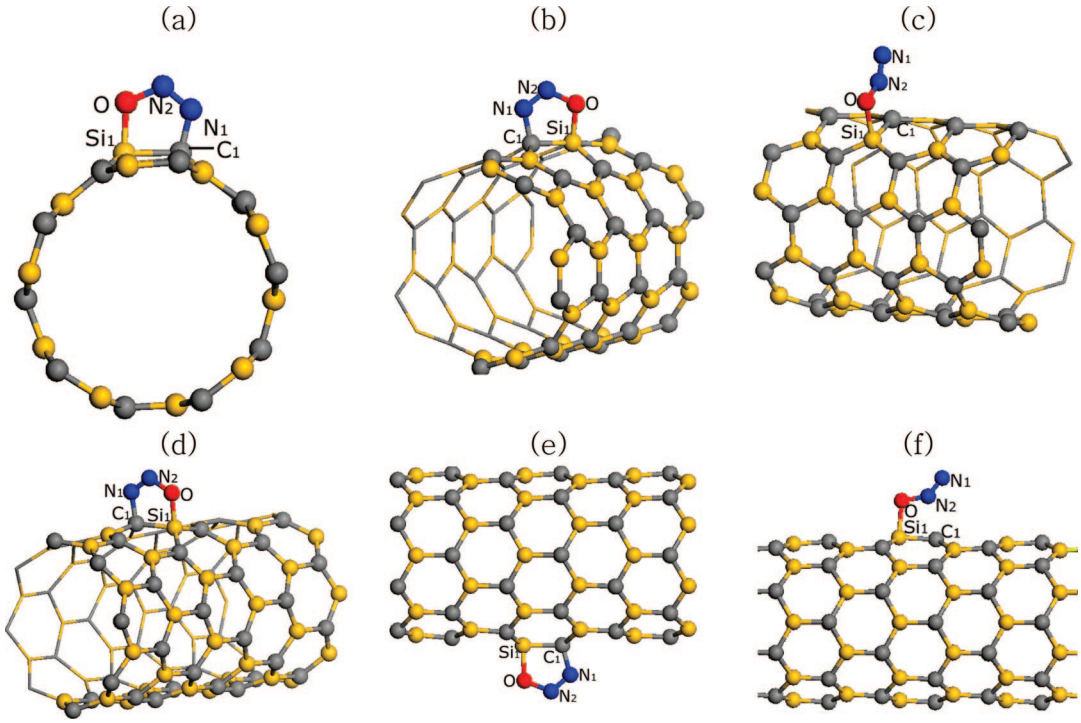

Figure 7. Optimized structures for various configurations of SiCNT-NNO complexes: configurations E (a), Z (b), and C (c) of the (5,5) complex and configurations Z (d), A (e), and C (f) of the (8,0) complex. Atomic labels are also defined.

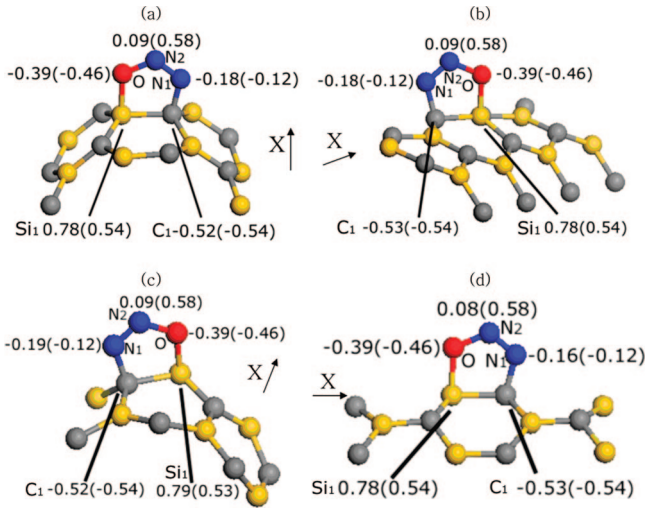

Figure 8. Mulliken charges of atoms around the adsorption site for SiCNT-NNO complexes depicted in Figure 7: configurations E (a) and Z (b) of the (5,5) tube and configurations Z (c) and A (d) of the (8,0) tube. All of them have the same orientations as in Figure 7.

orientation of the NNO molecule such that its molecular plane is perpendicular to the tube surface.

Figure 7(c) shows another configuration (C) in which the five-membered ring is not formed. Here, the NNO molecule adopts a different orientation with respect to the tube. Table 3 shows that this configuration is much less stable than others for both (5,5) and (8,0) SiCNTs. Indeed, the positive values of binding energy indicate that the configuration corresponds to a metastable state. Thus we do not consider it in further analyses.

Table 3 shows that lengths of the O−Si_1 and N_1−C_1 bonds are similar to the corresponding values in a stable SiCNT-

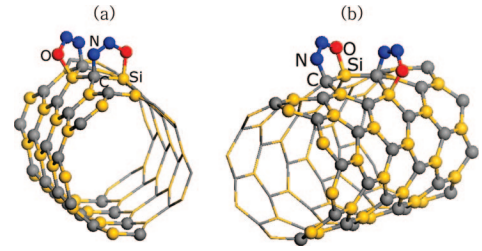

Figure 9. Optimized structures of (5,5) (a) and (8,0) (b) SiCNT-2NNO complexes.

NO complex. As already noted, the geometry of the NNO molecule shows a significant degree of deformation, as evidenced by large deviations in the N_1−N_2−O bond angle from 180°. In fact, the bond angle (∼117°) shown in the table indicates that N_2 is nearly sp^2-hybridized, which is achieved by its protrusion from the circumference of the tube. The N_1−N_2 and N_2−O bonds are elongated by different amounts in such a way that the molecule has N1═N2−O bonds. (We recall that the bond orders of N_1−N_2 and N_2−O bonds are 2.5 and 2 in an isolated NNO molecule.) The C_1−Si_1 bond is also elongated by an appreciable amount (∼0.17 Å) compared to that in pristine tubes. As shown in Table 3, Mulliken charge analysis shows a charge transfer (∼0.48*e*) from the tubes to the molecule, which is comparable to what is seen with the SiCNT-NO complex. Figure 8 shows a more detailed analysis of the Mulliken charges for atoms around the adsorption site. Comparing the charges on the atoms around the adsorption site with the corresponding values in the isolated molecule and tube shows that most of the transferred charge is concentrated on the central nitrogen atom, N_2, making it almost neutral. A careful analysis of the changes in charge on Si_1, N_2, and O upon complex formation shows that most of the charge transfer

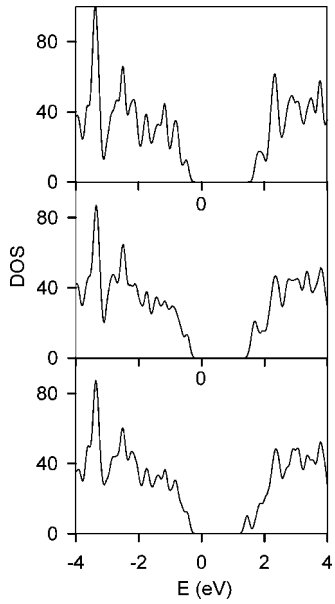

Figure 10. Comparison of the electronic density of states (DOS) for (5,5) SiCNT-NNO complexes: pristine tube (top), configuration E (middle), and configuration Z (bottom).

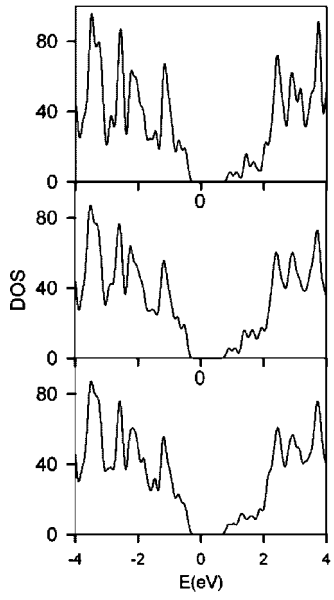

Figure 11. Comparison of the electronic density of states (DOS) for (8,0) SiCNT-NNO complexes: pristine tube (top), configuration Z (middle), and configuration A (bottom).

from the tube to the molecule occurs from Si_1 to N_2 through O, allowing N_2 to have an unpaired electron in one of its sp^2 hybrid orbitals. Another transfer route running from C_1 to N_2 through N_1 makes a much smaller contribution to the charge transfer.

Figure S6 shows four additional configurations (K1−K4) of the (5,5) SiCNT-NNO complex investigated, each of which has a local geometry similar to the corresponding one for the SiCNT-NO complex shown in Figure S3. Except configuration K1, all of them result in the physisorption with the binding energy less than −0.02 eV upon the relaxation of geometry. Optimization of configuration K1 results in configuration C shown in Figure 7(c). Figure S7 also shows additional configurations (L1−L4) of the (8,0) SiCNT-NNO complex. Similar to the case of their correspondents for the (5,5) complex, all of them exhibit physisorption with the binding energy less than −0.01 eV except configuration L1. Optimization of configuration L1 also results in configuration C shown in Figure 7(f).

We have also investigated the physicochemical properties of SiCNTs when two NNO molecules are adsorbed on the surface. In order to do this, we take configurations E of the (5,5) SiCNT-NNO complex and A of the (8,0) complex, which are the most stable ones when one NO molecule is adsorbed. We also find that two NNO molecules tend to bind to adjacent sites rather than being far apart, as evidenced by the difference in the binding energy of 0.12 eV and 0.10 eV for (5,5) tube (8,0) tube, respectively. Figure 9 shows that the (5,5) SiCNT-2NNO complex adopts E and Z configurations, while the (8,0) complex adopts Z and A configurations of the two molecules. In addition, the adsorption is also cooperative. For the (5,5) tube, the binding energy of the first and the second molecule is −0.44 eV and −0.68 eV, respectively. For the (8,0) tube, the corresponding value is −0.56 eV and −0.72 eV, respectively.

Figures 10 and 11show that the electronic density of states (DOS) for stable configurations of SiCNTs does not differ much from that of the pristine tube near the Fermi level. One may note that the band gap decreases slightly (<0.2 eV) upon adsorption. In addition, there is little shift in the Fermi level after adsorption, indicating that the rigid charge transfer model does not apply to this system. A separate analysis shows that the top of the valence band is mostly composed of π states of the tube in which electron densities are concentrated on carbon atoms. Doubly degenerate HOMOs of the isolated NNO molecule, which split into σ and π states upon adsorption on the tube, do not affect the electronic structure of the complex at the top of the valence band, since they are located more than 1.8 eV below the Fermi level. Likewise, doubly degenerate LUMOs of the NNO molecule also interact with conduction bands at 0.3 eV above their bottom. Figures S8 and S9 show band structures of the (5,5) and (8,0) complexes as the number of adsorbed molecules are varied.

Table 4shows that the adsorption of the NNO molecule on the surface of CNTs or BNNTs is also unfavorable, as indicated by significantly positive values of the binding energy. Once adsorbed, the geometry of the adsorbed complex is similar to that of the corresponding SiCNT-NNO complex, in that five-membered rings are formed at the adsorption site.

4. Conclusions

Using a theoretical method based on first principles, we have investigated the chemisorptions of NO and NNO molecules on SiCNTs, CNTs, and BNNTs. To the authors' knowledge, this is the first theoretical work examining the possibility of chemisorbing the notorious nitrogen oxide pollutants on these nanotubes in detail. Our calculations show that they can be adsorbed on silicon carbide nanotubes (SiCNTs) with an appreciable binding energy. A detailed investigation of energetics, electronic structure, and magnetic properties of the adsorbed complexes was made, which gives useful results for NOx sensing. On the other hand, chemisorptions on carbon nanotubes (CNTs) or boron nitride nanotubes (BNNTs) are severely

Table 4. Energetic and Geometric Parameters for Various Configurations of CNT-NNO and BNNT-NNO Complexes in Which the Nanotubes Have (5,5) and (8,0) Chiral Indices

	CNT				BNNT			
	(5,5)[g]		(8,0)[g]		(5,5)[g]		(8,0)[g]	
configuration	E	Z	Z	A	E	Z	Z	A
E_b[a] (eV)	1.70	1.50	1.58	1.07	1.50	no binding	no binding	1.29
l (O−C_1)[b] (Å)	1.54 (1.75)	1.51 (1.74)	1.53 (1.75)	1.49 (1.74)	1.59 (1.75)			1.56 (1.74)
l (N_1−C_2)[c] (Å)	1.57 (1.52)	1.55 (1.52)	1.57 (1.52)	1.52 (1.51)	1.64 (1.52)			1.63 (1.51)
l (O−N_2)[d] (Å)	1.37 (1.20)	1.40 (1.20)	1.38 (1.20)	1.40 (1.20)	1.32 (1.20)			1.33 (1.20)
l (N_1−N_2)[e] (Å)	1.23 (1.15)	1.23 (1.15)	1.23 (1.15)	1.23 (1.15)	1.23 (1.15)			1.23 (1.15)
θ(N_1−N_2−O)[f]	116.3 (180)	114.6 (180)	115.3 (180)	114.4 (180)	119.9 (180)			119.4 (180)

[a] Binding energy of one NNO molecule on the surface of the CNT or BNNT. [b] O−C_1 distance, where C_1 is the carbon atom of the CNT above which O is located. In the BNNT, C_1 represents a boron atom of the tube. [c] N_1−C_2 distance, where C_2 is the carbon atom of the CNT above which N_1 is located. In the BNNT, C_2 represents a nitrogen atom of the tube. Two nitrogen atoms of the NNO molecule are defined by the bonds N_1−N_2−O. [d] N_2−O bond length of the NNO molecule. The numbers in parentheses denote the corresponding data in an isolated molecule. See footnote *c* for the definition of N_2. [e] N_1−N_2 bond length of the NNO molecule. The numbers in parentheses denote the corresponding data in an isolated molecule. See footnote *c* for the definitions of N_1 and N_2. [f] Bond angle of the NNO molecule. [g] Chiral index.

endothermic, resulting in metastable complexes. In some cases, not even these metastable states are predicted to exist. In conjunction with Rafati et al. result on the physisorption of the NO molecule on CNTs, these results suggest that only SiCNTs would be practically useful for the removal of NO and NNO molecules among three nanotubes. Change of magnetic properties will be particularly useful for sensing the amount of NO molecules adsorbed on SiCNTs.

Acknowledgment. This work was supported by a Korea Research Foundation Grant funded by the Korean Government (MOEHRD) (KRF-2007-313-C00334), in which the main calculations were performed using the supercomputing resource of the Korea Institute of Science and Technology Information (KISTI).

Supporting Information Available: Figures S1−S9. This material is available free of charge via the Internet at http://pubs.acs.org.

References

(1) Janzen, E.; Kordina, O.; Henry, A.; Chen, W. M.; Son, N. T.; Monemar, B.; Sorman, E.; Berganman, P.; Harris, C. I.; Yakimova, R.; Tuominen, M.; Konstantinov, A. O.; Hallin, C.; Hemmingsson, C. *Phys. Scr.* **1994**, *T54*, 283.

(2) Sun, X.-H.; Li, C.-P.; Wong, W.-K.; Wong, N.-B.; Lee, C.-S.; Lee, S.-T.; Teo, B.-K. *J. Am. Chem. Soc.* **2002**, *124*, 14464.

(3) (a) Menon, M.; Richter, E.; Mavrandonakis, A.; Froudakis, G.; Andriotis, A. N. *Phys. Rev. B* **2004**, *69*, 115322. (b) Miyamoto, Y.; Yu, B. D. *Appl. Phys. Lett.* **2002**, *80*, 586. (c) Mavrandonakis, A.; Froudakis, G. E.; Schnell, M.; Muhlhauser, M. *Nano Lett.* **2003**, *3*, 1481.

(4) Zhao, J.-x.; Ding, Y.-b. *J. Phys. Chem. C* **2008**, *112*, 2558.

(5) Mopurmpakis, G.; Froudakis, E.; Lithoxoos, G. P.; Samios, J. *Nano Lett.* **2006**, *6*, 1581.

(6) Zel'dovich, Ya. B.; Sadovnikov, P. Ya.; Frank-Kamenetskii, D. A. *Oxidation of Nitrogen in Combustion*; Acad. of Sci. USSR: Moscow, 1947.

(7) Shelef, M. *Chem. Rev.* **1995**, *95*, 209.

(8) McCue, J. T.; Ying, J. Y. *Chem. Mater.* **2007**, *19*, 1009.

(9) Boon, E. M.; Marletta, M. A. *J. Am. Chem. Soc.* **2006**, *128*, 10022.

(10) Huang, Y.; Ho, W.; Lee, S.; Zhang, L.; Li, G.; Yu, J. C. *Langmuir* **2008**, *24*, 3510.

(11) Rafati, A. A.; Hashemianzadeh, S. M.; Nojini, Z. B. *J. Phys. Chem. C* **2008**, *112*, 3597.

(12) Chen, H.-T.; Musaev, D. G.; Irle, S.; Lin, M. C. *J. Phys. Chem. A* **2007**, *111*, 982.

(13) Gronbeck, H.; Hellman, A.; Gavrin, A. *J. Phys. Chem. A* **2007**, *111*, 6062.

(14) (a) Broqvist, P.; Panas, H.; Fridell, E.; Persson, H. J. *Phys. Chem. B* **2002**, *106*, 137. (b) Schneider, W. F.; Hass, K. C.; Miletic, M.; Gland, J. L. *J. Phys. Chem. B* **2002**, *106*, 7405. (c) Miletic, M.; Gland, J. L.; Hass, K. C.; Schneider, W. F. *J. Phys. Chem. B* **2003**, *107*, 157. (d) Karlsen, E. J.; Nygren, M. A.; Petterson, G. M. *J. Phys. Chem. B* **2003**, *107*, 7795. (e) Broqvist, P.; Gronbeck, H.; Fridell, E.; Panas, I. *J. Phys. Chem. B* **2004**, *108*, 3523. (f) Xu, S. C.; Irle, S.; Musaev, D. G.; Lin, M. C. J. *Phys. Chem. B* **2006**, *110*, 21135.

(15) Kresse, G.; Hafner, *Phys. Rev. B* **1993**, *47*, 558.

(16) Kresse, G.; Joubert, D. *Phys. Rev. B* **1999**, *59*, 1758.

(17) Kresse, G.; Furthmuller, J. *Phys. Rev. B* **1996**, *54*, 11169.

(18) Perdew, J. P.; Burke, K.; Ernzerhof, M. *Phys. Rev. Lett.* **1996**, *77*, 3865.

(19) Throughout this work, the accuracy of calculations on the electronic LDOS was carefully confirmed by separate band structure calculation.

(20) Huheey, J. E.; Keiter, E. A.; Keiter, R. L. *Inorganic Chemistry*, 4th ed.; HarperCollins College Publishing: New York, 1993; Chapter A-28.

CT800273C